Multi-agent simulation of benthic foraminifera response to annual variability of feeding fluxes

Maciej Komosinski[a,*], Agnieszka Mensfelt[a], Jarosław Tyszka[b], Jan Goleń[b]

[a] *Institute of Computing Science, Poznan University of Technology, Piotrowo 2, 60-965 Poznan, Poland*
[b] *ING PAN – Institute of Geological Sciences, Polish Academy of Sciences, Research Center in Kraków, BioGeosystem Modelling Laboratory, Senacka 1, 31-002 Kraków, Poland*

Abstract

In this work we describe a novel simulation model of foraminifera and their microhabitat. The simulations reported here are focused on the response of foraminiferal populations to environmental feeding fluxes. The experiments allowed to calibrate the model and to simulate realistic population patterns known from culture experiments, as well as from oceanographic and paleoecologic studies. Variability of annual food flux has a direct impact on productivity of foraminifera: population sizes closely follow the intensity of constant and seasonal food fluxes in both scenarios. This correlation between the food influx and population size is interpreted as the consequence of changing the carrying capacity of the system. Seasonal pulses of particulate organic matter enhance the population size which is represented by a higher number of fossilized shells. Our model offers a flexible experimental design to run sophisticated *in silico* experiments. This approach reveals a novel methodology for testing sensitivity of fossil and recent foraminiferal assemblages to environmental changes. Furthermore, it facilitates predictive applications for monitoring studies based on simulation of various scenarios.

Keywords: Foraminifera, simulation, population dynamics, life cycles, seasonality

1. Introduction

This work introduces a multi-agent simulation model of Foraminifera and their microhabitat (Fig. 1). Artificial life methodology [1, 2] is employed to develop an *in-silico* software model that is continuously improved and calibrated for reconstruction and prediction of various short- and long-term processes of foraminifera, including their behavior (Fig. 2), population dynamics, life-history strategies, energy flow, as well as selected evolutionary phenomena.

Foraminifera are ideal model organisms often used for testing paleoecological and evolutionary hypotheses (e.g. [3, 4]). They are single-celled eukaryotes that populate marine benthic and pelagic zones throughout the world [5, 6, 7]. Foraminifera have an extraordinary fossil record at least since the Cambrian (500 million years ago) [8, 7]. Most foraminifers produce diverse shells, covering their soft cells. Foraminifera with spheroidal (globular) chambers that belong to the class Globothalamea [9] represent the main focus of our investigations.

*Corresponding author
Email addresses: maciej.komosinski@cs.put.poznan.pl (Maciej Komosinski), agnieszka.mensfelt@cs.put.poznan.pl (Agnieszka Mensfelt), ndtyszka@cyf-kr.edu.pl (Jarosław Tyszka), ndgolen@cyf-kr.edu.pl (Jan Goleń)

This paper appeared in *Journal of Computational Science*, 2016.
http://dx.doi.org/10.1016/j.jocs.2016.09.009

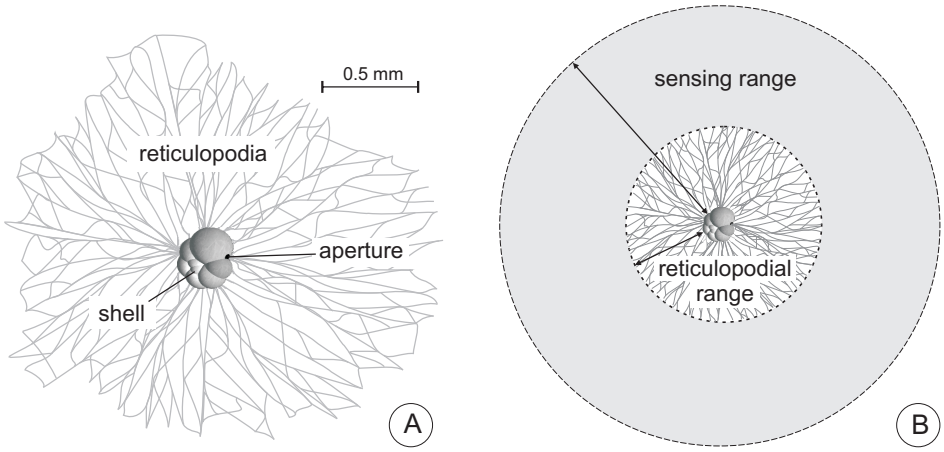

Figure 1: A foraminifer with its reticulopodia. (A) A single individual with extended reticulopodia during searching and feeding behavior. (B) A model of an agent with the circular reticulopodia range surrounded by the chemotactic sensing range.

This study follows morphogenetic models developed to simulate diverse patterns of foraminiferal shells that grow by successive additions of chambers [10, 11, 12]. It extends these models to agent population models by introducing foraminiferal behavior, energy flow, and life cycles for realistic simulations of population dynamics and evolutionary processes (see [13, 14, 15] for further explanation of the eVolutus project).

Benthic foraminifera mainly feed on particulate organic matter (POM), thus they are strongly dependent on POM availability in time and space [6, 7, 16, 17]. Seasonality (e.g., nutrient availability, light and temperature) is the most conspicuous temporal variability that influences POM flux. The POM flux and its variability have a direct impact on distribution, life history strategies, reproduction, and population dynamics of foraminifera [18, 6, 17].

A life span in foraminifera ranges from a few weeks to a few years [19, 18]. Although life cycles with three generations are frequent in benthic foraminifera, a typical life cycle is characterized by an alternation of two modes of reproduction: sexual (in the haploid generation) and asexual (in the diploid generation) [19] (Fig. 3). This life cycle helps foraminifera adjust to variable environmental conditions by generating diverse and flexible life history strategies [6].

The main objectives of this study include: (1) defining and calibration of model parameters; (2) designing and running feeding experiments that test a response of foraminiferal life cycles to variability of feeding fluxes. We test the flexibility of such life strategies to aseasonal vs. seasonal organic matter fluxes.

1.1. Simulation software

For simulation experiments we use Framsticks [20, 21], a highly configurable and versatile simulation toolkit. This software environment has been earlier used for modeling complex collective systems, autonomous agents, and evolutionary and co-evolutionary processes. It allows for an arbitrary number of genetic encodings and their hierarchy [22, 23] and two modes of mechanical simulation (accurate rigid body and approximate elastic body) [24, 25, 26]. Framsticks features a custom scripting language, FramScript, that is tailored for the

development of various artificial life experiments. Most aspects of the simulation and the user interface can be defined by scripts. The simulator is available for both desktop and mobile devices and provides a number of user interfaces, from simple graphical ones to advanced command-line and distributed client-server architectures.

2. Parametrization of foraminifera and their microhabitat

This section discusses key parameters of our simulation model.

2.1. Environment and agent behavior

Sea floor area. A 10 cm × 10 cm square represents a small 100 cm^2 area of the sea floor populated by virtual benthic foraminifera. The benthic habitat in reality is 3-dimensional because foraminifera live within an approximately 10 cm layer of soft marine sediment [6, 27, 7]. This virtual space is reduced to two-dimensions to avoid implementation of additional interactions present within the sediment [28]. This surface may represent a sediment/water interface populated by an assemblage of epibenthic (epifaunal) foraminifera. Mobile epifaunal foraminifera are most sensitive to organic matter fluxes [27, 16, 28].

Reticulopodia range. Granuloreticulopodia are anastomosing networks of pseudopodia extended by foraminifers through either single or multiple apertures to monitor the microhabitat, gather food, attach, and move, as well as to transmit environmental and intracellular signals [6, 29, 18] (Fig. 1). In consequence, reticulopodia that extend radially from the shell match the circular range that has physiologic and mechanistic limits. The maximum reticulopodial range for small foraminifers (0.1 to 0.5 mm in diameter) may be several times larger than the diameter of shells [30, 29]. We arbitrarily set this value to 1 mm (Fig. 1).

Sensing range. Most bacteria and many eukaryotic cells respond to chemotactic stimuli that depend on their threshold concentration and the saturating concentration [31, 32]. Food signals, i.e. chemical signals diffused around organic particles, seem to be essential for most organisms. Such positive signals might give directions for active movement [32]. Reticulopodia directly monitor the circular area around the shell. However, the sensing distance has never been measured. Nevertheless, it is very likely that they are also able to recognize chemotactic signals supposed based on the observation of straight movement of grazing epiphytic foraminifera towards densely colonized bacterial and fungal substrates [33]. Thus, the external limit of sensing range in simulated individuals, calculated as the distance from the shell, is arbitrarily set at 3 mm (Fig. 1).

Other combinations of reticulopodia and sensing ranges have been tested in earlier simulations [14].

Locomotion of foraminifera. Kitazato [34] analyzed the velocity of movement of 22 species of benthic foraminifera that ranged from 0.008 to 0.082 mm/min. Vagile epifaunal individuals moved faster than infaunal (endobenthic) ones. Recent observations [35] place average speeds in the upper part of this range, 0.07 to 0.08 mm/min. Thus, the speed between 0.05 and 0.1 mm/min seems to be realistic. We arbitrarily set the speed value at 0.05 mm/min. for all individuals to simplify the model and focus on the influence of other parameters. It is important to point out that *in vivo* speed experiments consider the movement on a glass surface [34, 35] which overestimates the speed. Furthermore, all velocities were calculated based on the net distance traveled by a specimen, i.e. the shortest distance between the starting and the ending points of a complex trajectory of movement (see comments in [36]).

Movement strategy. When food particles are outside of the chemotactic sensing range (Fig. 2), an agent moves in random directions. When a food particle is within the sensing

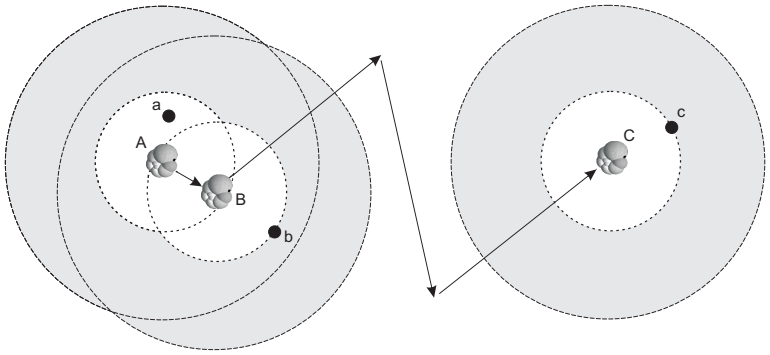

Figure 2: A model of foraminiferal behavior that represents searching, sensing, feeding, and movement activities. When a food particle (a) falls into the white reticulopodia range of (A), it is collected and eaten. When a food particle (b) is within the gray sensing range of (A), a foraminifer has to move towards food. The particle is collected if the external limit of reticulopodia can reach it (B). When there is no food available, a foraminifer starts moving in a random direction, periodically changing directions (C). This strategy allows collecting particles (c) that are initially outside of both ranges.

range, an agent moves directly towards this particle until it touches the particle with its reticulopodia. Other behavioral strategies can also be implemented in the future.

Direction change period. In the simulation, a foraminifer changes direction periodically when no nutrient is sensed. This period is set arbitrarily to 100 minutes which results in direction changes every 5 mm.

2.2. Energy

We assume that energy stored by an organism is proportional to its body size that is represented by biomass [37]. In unicellular organisms, body size is the cell volume that can be considered as the volume of protoplasm (i.e., cytoplasm with the nucleus). The protoplasm quality, translated to its energetic value, varies depending on its molecular composition. Nevertheless, for the sake of simplicity at this stage of model development, a constant energetic value of the protoplasm is chosen. Consequently, the starting energy of a single foraminifer agent is proportional to the volume of the proloculus:

$$starting\_energy = carbon\_per\_protoplasm\_ratio \cdot \frac{4}{3}\pi r^3 \text{ [pg]} \tag{1}$$

We arbitrarily set the carbon per protoplasm ratio at 0.13 pg/μm^3. Following Putt and Stoecker [37], organic carbon per protoplasm volume ratio ranges from 0.07 to 0.19 picograms of C_{org} per 1 μm^3 which gives 70 to 190 micrograms of C_{org} in 1 mm^3 of protoplasm.

The radius of the first chamber called the proloculus ($chamber\_radius_1$) is 20 μm in case of haploids and 10 μm in case of diploids. The radius of each of the subsequent chambers is calculated as:

$$chamber\_radius_{i+1} = 1.07 \cdot chamber\_radius_i \tag{2}$$

This formula follows the growth factor (sensu [38, 10, 12]) that is the ratio between the radii of two successive chambers. A new chamber in an agent shell is grown when the amount of the accumulated energy exceeds the volume capacity of all existing chambers.

Minimal energy of a haploid proloculus. Proloculus is the first chamber of the shell in multichambered foraminifera. It is more or less spherical in shape. The haploid generation

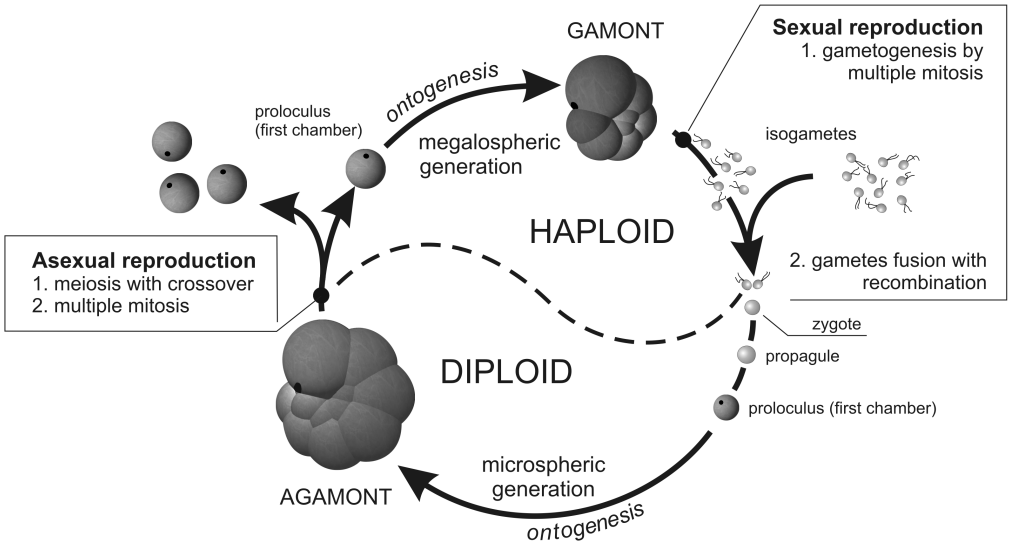

Figure 3: Benthic foraminifera life cycle with bimorphic generations and two reproduction modes (modified after [19]). This cycle is introduced into the presented model.

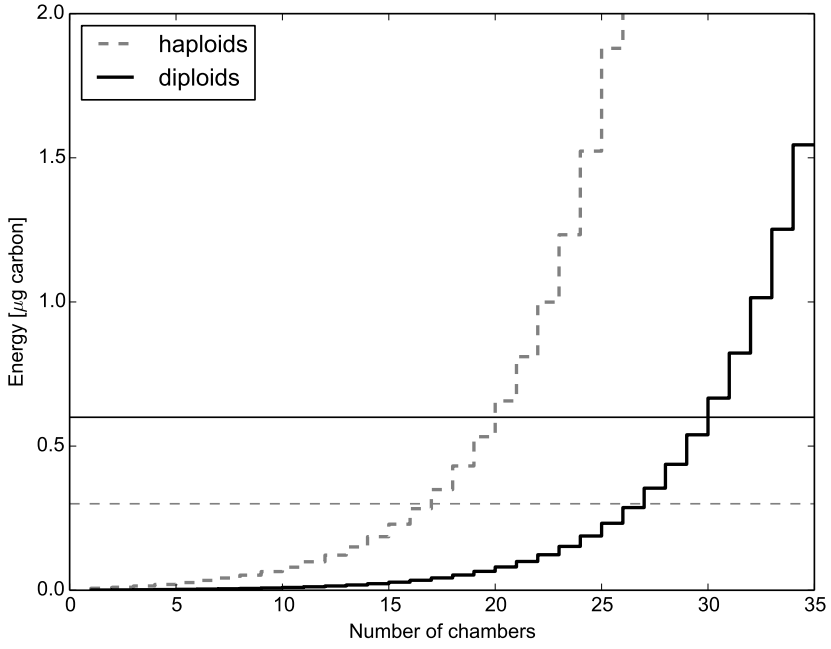

Figure 4: The maximal amount of energy that can be stored by a simulated individual with the given number of chambers. Horizontal lines are the maturation checkpoints of haploids and diploids.

in foraminifera tends to have a larger proloculus than the diploid one [39, 5]. In consequence, the haploid generation is also called megalospheric. The range of proloculus diameter in haploid foraminifera may vary on average from 30 to 80 μm [40, 6]. We set the haploid proloculus radius to 20 μm. According to (1), the starting energy of such a chamber is equal to 4355 pg C_{org}.

Minimal energy of a diploid zygote. Diploids that represent the microspheric foraminiferal generation are formed after sexual reproduction by fusing two gametes of the same species [41, 19]. The radius of gametes in different species of foraminifera ranges from about 0.55 to 2 μm [42, 43]. The volume of a zygote is the sum of volume of the gametes that have been fused. In case of foraminifera, gametes have equal sizes and they are approximately spherical. In our model, a sphere (a zygote) that represents successfully fused gametes has the radius of 1.25 μm. According to (1), it contains 1.06 pg C_{org}.

Minimal energy of a diploid proloculus. The diploid proloculus is often smaller than the haploid one. Nonetheless, it is still much larger than the initial zygote stage of an individual. Following recent indirect conclusions from culture studies [44, 45], this naked stage lacking any shell is called a propagule (Fig. 3). The first chamber in our model has the radius of 10 μm and consists of 544.54 pg C_{org}. The difference between the zygote energy value and the proloculus value has to be ingested from the microhabitat. The propagules are able to colonize new habitats and to switch to a dormancy stage when they encounter unfavorable conditions [44, 45].

Haploid maturation checkpoint. This parameter defines the amount of energy which has to be accumulated by a haploid individual before maturation. When the threshold of assimilated organic carbon (300 000 pg C_{org}) is exceeded, the agent may reproduce sexually by gametogenesis.

Diploid maturation checkpoint. This maturation checkpoint is defined as the energy threshold for reproduction of diploid individuals. When this threshold (600 000 pg C_{org}) is exceeded, the agent may reproduce asexually by a single meiosis followed by multiple mitosis.

Nutrient energy. The energy contained in one nutrient item is 108 908 pg C_{org}, and in the simulation nutrients are considered point particles.

Feeding flux. We have performed the experiments with different values of this parameter. The supply of nutrients in one group of simulations was constant and in the other it was changing seasonally. The details are described in Sect. 3.2.

Energy transfer rate. Energy transferred from nutrient to foraminifer per second is calculated as:

$$energy\_transferred = min(energy\_transfer\_rate \cdot current\_energy, nutrient\_energy) \text{ [pg/s]} \quad (3)$$

We performed simulation experiments with $energy\_transfer\_rate = 0.001$ and 0.0001, and we assumed that C_{org} ingestion rate is proportional to the body size that is represented by the current energy contents. This means that smaller individuals (agents) transfer energy, i.e. C_{org}, slower than larger ones.

Normal energy usage. We define the normal energy usage at the stage when the main agent activities include reticulopodial monitoring and sensing. This is in contrast to the dormancy stage when reticulopodia are withdrawn and all activities are limited to sensing. Energy used per second is equal to 0.00005% of the current energy of an agent.

Energy used for movement. Foraminiferal locomotion is energetically demanding because it is based on complex interactions between cytoskeletal structures, motor and associated proteins [29]. Nevertheless, energetic cost of movement in foraminifera has not been estimated. According to Hannah et al. [46], benthic foraminifera respires ten times more

rapidly than naked amoebae of comparable size. In consequence, a high degree of respiration is associated with the acquisition of food resources [46] that is done by extensive reticulopodial activity, including movement [29]. Granuloreticulopodia in foraminifera are rich in mitochondria that constitute a large part of bidirectionally moving granules [29]. This also confirms high costs of motility that is massively fueled by ATP produced and distributed by mitochondria (compare [47]). We set energy used for movement per second as 0.00005% of the maximum amount of energy an agent ever gathered.

Energy used for chamber growth. Cell (body) growth in multichambered foraminifera is associated with shell growth by iterative construction of successive chambers [6, 7]. We set energy used for chamber growth per second to 0.0001% of the current energy of an agent. This is an arbitrary value because the energetics of chamber formation has never been measured experimentally.

Chamber formation period. The process of chamber formation in Globothalamea takes from 8 to 24 hours [48, 19, 18]. Smaller, more opportunistic foraminifera tend to construct chambers faster, and this process takes from 8 to 12 hours. It is therefore assumed that chamber formation in simulations takes 12 hours. During chamber formation, globothalamean foraminifera have to stop all activities associated with reticulopodial searching, feeding, and movement [48, 19, 18].

Efficiency of energy usage. A cell is a thermodynamic machine that requires a steady supply of energy for conversion into useful work that is done with some level of efficiency [49]. The efficiency of such a machine is defined as the ratio of power output to power input [49] and depends on the genetically coded quality of the "cellular machine" and the quality of fuel (food) within the context of habitat conditions. "The degree of coupling of both subsystems" (sensu [49]) is essential for optimal conversion and efficiency of the system. Therefore, the efficiency of an agent (a cell) depends on intrinsic (mainly genetic) and extrinsic (environmental) factors.

The overall efficiency of molecular "engines" in living cells is estimated to be about 20% [49]. According to Lee et al. [50], conversion of ingested food, calculated as carbon, into body tissue is relatively small and depends on the ontogenetic stage of foraminifers. The youngest individuals convert from 10.75% to 21.58% of ingested carbon. This value is called the ecological growth efficiency defined as the ratio P/I between production P and ingestion I [50].

We arbitrarily set the efficiency of energy usage at 25%, thus 75% of the nutrient energy is assumed to be lost for energy slippage, including heat and molecular wastes as well as leaking membranes and channels.

Success of fertilization. There are no available data on gametes fusion rate for foraminifera. An individual success of external fertilization depends on population density [51] and water motion [52]. It has been empirically tested that for sea urchins, the success of fertilization can vary from 0% to 82% [51]. This parameter for sea urchins as well as for other multicellular organisms tells us how many released eggs become fertilized. Foraminifera reproduce sexually by isogamy [19], thus, they produce identical gametes of equal size, so this parameter should be defined as a fraction of all released gametes which undergo fusion. It is therefore most likely a very low value. We set it arbitrarily to 0.1% of gametes that succeed in forming zygotes.

Energy used for reproduction of a haploid. The energetic cost of multiple mitosis during sexual reproduction in foraminifera has never been estimated. Following experimental data based on cancer cells [53] and assumptions presented by Hecht et al. [47], the cost of mitosis is approximated at 0.0000007 J per single mitotic event. This value corresponds to 20 pg C_{org}. If we consider the smallest reproduced haploid consisting of 300 000 pg C_{org}, it will need nearly 54.6% of its energy to produce $2^{13} = 8192$ gametes in 13 cycles of multiple

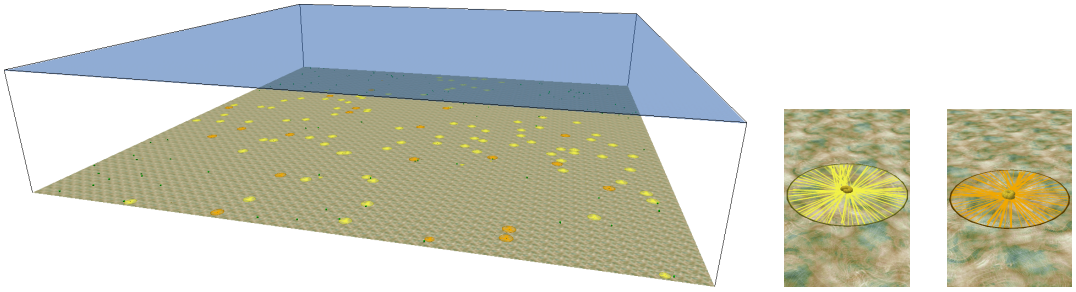

Figure 5: A sample view of the simulation with brighter (yellow) and darker (orange) circles depicting reticulopodial ranges of haploid and diploid individuals, respectively. This screenshot comes from the "Artificial Life" application that is a part of the Framsticks distribution [56]. A short video illustrating the simulation, generated with the raytracing rendering technique, is available at https://www.youtube.com/watch?v=2JrV2NmYu3U.

mitotic events.

In our model, we assume that each division splits the amount of available energy perfectly equally. This is why the number of offspring is always 2^n, and this number may be very sensitive to the initial amount of energy (in a specific case, a tiny modification of initial energy may change the number of offspring between 2^n and 2^{n+1}). Unequal and potentially randomized division of energy could be allowed to avoid such abrupt, discrete changes. Although there is no empirical data available, our experiments in the future will test the influence of non-perfect division of energy.

Energy used for diploid reproduction per single mitotic event is equal to 20 pg C_{org}. If we consider the smallest reproduced diploid consisting of 600 000 pg C_{org}, it will need nearly 0.85% of its energy to produce $2^8 = 256$ offspring in 8 cycles of multiple mitotic events. Diploids undergo a single meiotic division that is approximated as a double mitotic event at 40 pg C_{org}. We assume that meiosis precedes multiple mitosis because this strategy saves energy for reproduction.

Probability of sexual reproduction. We assume that reproduction is not completely deterministic – every five minutes, a haploid individual that reached the reproduction threshold (maturation checkpoint) may become ready for reproduction with probability 80%.

Reproduction period for haploids. In our model, gametes are released simultaneously. Every 720 seconds, haploids which are ready for reproduction reproduce with the probability mentioned in the previous paragraph. In nature, similar phenomena may be linked to lunar cycles [54]. Their biological function enhances the success of fertilization [55].

Minimal energy. Minimal energy level necessary for living is calculated as

$$minimal\_energy = minimal\_energy\_fraction \cdot maximum\_energy \tag{4}$$

This parameter defines how much energy a foraminifer can lose before it dies of starvation. We assume that this equals half of the maximal amount of energy achieved during the life of an agent ($minimal\_energy\_fraction = 0.5$).

Table 1 summarizes major parameters and their values that have been discussed in detail above.

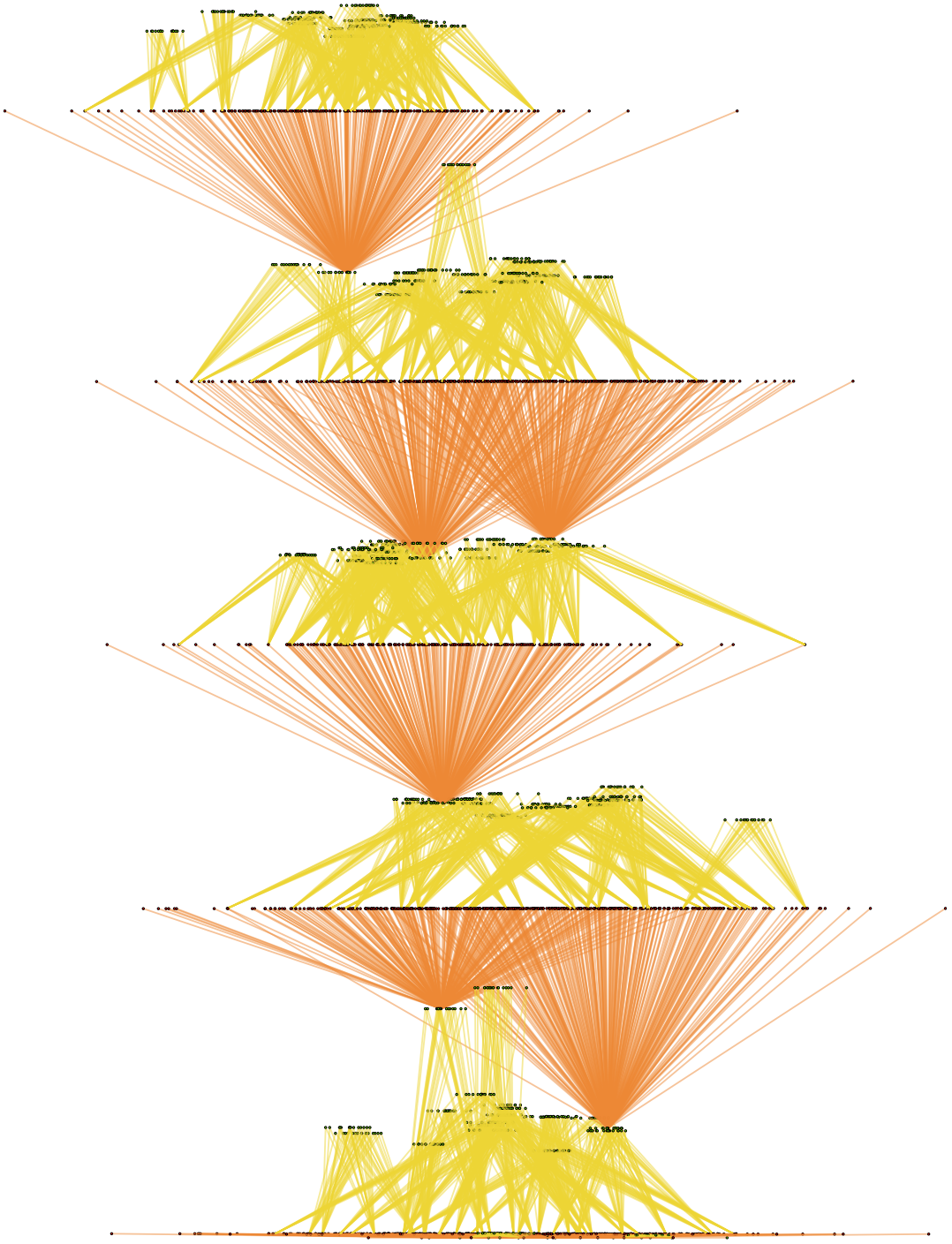

Figure 6: A genealogical tree that illustrates inheritance relationships between individuals during simulation. The vertical axis is simulation time (starts at the bottom). Green dots represent diploid generations, and red dots represent haploid generations. Lines correspond to a transfer of genetic information between generations. Orange lines illustrate asexual reproduction of diploid microspheric individuals (green dots) to megalospheric haploids (red dots). Yellow lines represent a sexual fusion of two haploid gametes into a diploid zygote.

Parameter	Value in simulation
Sea floor area	100 cm^2
Movement speed	0.05 mm/minute
Direction change period	100 minutes
Chamber formation period	12 hours
Reticulopodia range	1 mm
Sensing range	3 mm
Minimal energy of a haploid proloculus	4355 pg
Minimal energy of a diploid zygote	1.06 pg
Minimal energy of a diploid proloculus	544.54 pg
Haploid maturation checkpoint	300 000 pg
Diploid maturation checkpoint	600 000 pg
Minimal energy fraction needed to survive	0.5
Nutrient energy	108 908 pg
Feeding flux	**variable**
Feeding flux mode	**constant** or **seasonal**
Energy transfer rate	**0.001** or **0.0001**
Energy used per second	0.00005%
Energy used for movement per second	0.00005%
Energy used for chamber growth per second	0.0001%
Efficiency of energy usage	25%
Energy used per single mitosis	20 pg
Probability of reproduction	0.8
Reproduction period for haploids	720 s
Success of fertilization	0.1%

Table 1: Summary of major parameters used in foraminifera simulation and their selected values.

3. Simulation experiments

The experiments were performed according to the parameters described in the previous section. Fig. 5 presents a screenshot of a running simulation. In each simulation, time steps are discrete, but space is continuous (technically, coordinates are represented by floating point numbers). In each step agents move, dissipate energy, and die when their energy level drops below the minimal energy level.

Fig. 6 shows a genealogical tree constructed from the experiment with a constant feeding flux equal to 392.07 μg C_{org}per month. The feeding flux mode is analogous to the experiments depicted in Fig. 9 (A, B) and Fig. 10 (A, B). The tree presents 10 generations (nearly 6 years) and consists of 3082 haploid and 2805 diploid individuals. In the beginning of the simulation, the energies of the initial organisms are assigned randomly. The proliferation of the first diploid generation and the first two haploid generations occurred at very short intervals, as demonstrated by the nearly horizontal orange and yellow lines at the bottom. Then, after reaching the maturation checkpoint, two diploid individuals reproduced (orange lines) creating $2 \times 2^8 = 512$ haploid offspring. Young haploids dominate other individuals causing the alternation of generations. This phenomenon is also present in other simulation experiments (see Figs. 9 (A) and 10 (C)) – it will be illustrated and discussed in detail in the following subsections.

3.1. The influence of energy constraints on reproduction

Fig. 7 aggregates results of simulation experiments regarding the influence of proloculus size and maturation checkpoint on reproduction. They have been averaged from 10 simulation runs. In each simulation run, the feeding flux was constant and equal to 392.07 μg C_{org}

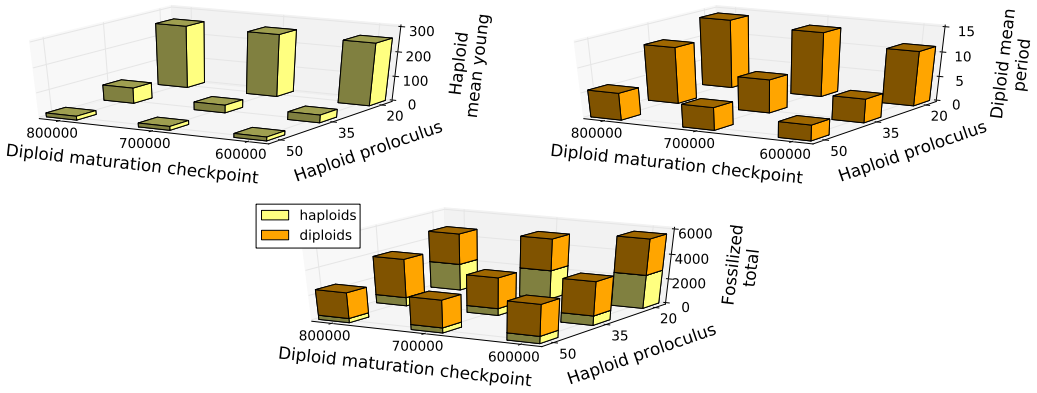

Figure 7: Top left: mean number of young haploids. Top right: mean period of diploid reproduction events (in months). Bottom: total fossilized shells during 10 years for different haploid proloculus radii (μm) and different diploid maturation checkpoints (pg C_{org}).

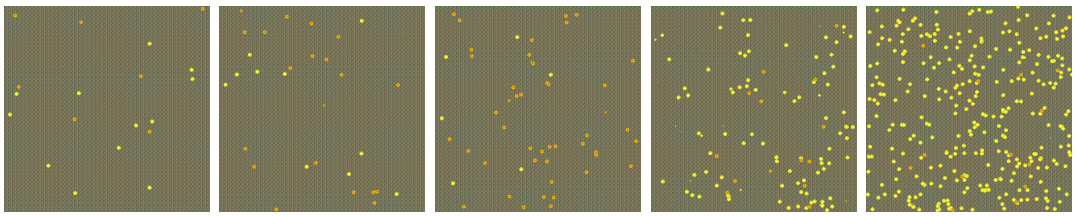

(a) initial state of the simulation (b) low season (c) low season, after reproduction event (d) initial month of the high season (e) high season

Figure 8: The number of foraminifera in the 100 cm^2 area of the sea floor. Nutrient supply is seasonal with high season (feeding flux=261.38) lasting 3 months and low season (feeding flux=43.56) lasting 9 months. These are different stages of an experiment with seasonality of feeding flux described in Sect. 3.2. Circles demonstrate foraminifer reticulopodia ranges (yellow for haploids and orange for diploids).

per month (compare Table 2 and Fig. 11). There are more young haploids with megalospheric shells when their proloculus (first chamber) is smaller because, in the reproduction event, energy of the diploid parent is divided into smaller units. There are also more young haploids when the diploid maturation checkpoint (the asexual reproduction threshold) is higher, because the amount of energy that is divided is larger. Diploid reproduction events are more frequent when the maturation checkpoint (the reproduction threshold) is lower. Diploid reproduction events are also more frequent when the haploid proloculus is larger because haploids need less time to reach their maturation checkpoint and produce diploid offspring. Consequently, the mean interval between diploid reproduction events is also shorter. When the radius of haploid proloculus is 20 μm, the number haploids and diploids in the fossil record is similar, but for 35 and 50 μm radii, diploids are more frequent. In nature, all these variables (proloculus size, maturity checkpoints for certain generations, growth rate etc.) may influence life history strategies. Changes of these variable values may be adaptive under certain conditions.

3.2. Constant vs. seasonal feeding fluxes

Preconditions. We run four pairs of experiments that differed only in the total annual amount of particulate organic matter (POM flux). Each experiment within the pair had one of the two temporal variabilities of the POM flux that was either constant or seasonal

POM flux	**Values of POM flux per 100 cm^2 [μg C_{org}]**			
Annual total, per year:	1176.20	2352.40	4704.80	9409.60
Constant (12 months), per month:	98.02	196.04	392.07	784.10
High season (3 months), per month:	261.38	522.76	1045.52	2091.04
Low season (9 months), per month:	43.56	87.13	174.25	348.51

Table 2: Microgram C_{org} per year and the corresponding particulate organic matter fluxes for experiments with constant and seasonal feeding fluxes.

throughout the year. The energy of the single nutrient was equal to 108 908 pg. The number of nutrients per 10 cm^2 appearing during one month was in both experiments adjusted in order to obtain the same total amount of nutrients per year in both constant and seasonal flux conditions (Table 2). Values of energy fluxes reported here are expressed in units of weight of C_{org} per time, and implicitly per the entire simulated area (100 cm^2).

The experimental area – a square of 10 cm × 10 cm – is populated by the same species of benthic foraminifera represented by haploid (megalospheric) and diploid (microspheric) generations following all parameters described above. Emigrations and immigrations are not allowed, thus the system is closed for external exchange. All experiments simulate a period of 10 years.

In the beginning of each simulation, 20 initial foraminifers are set up, and each of them is randomly assigned to the haploid or diploid generation with the probability of 0.5, as shown in Fig. 8 (a). The energy of the initial foraminifer is drawn from the range [proloculus energy, reproduction checkpoint] with uniform probability. For all foraminifers, $energy\_transfer\_rate$ is 0.001.

Experiments with constant feeding flux. These experiments have a constant POM flux throughout the simulation time. Four values of the POM flux are tested and they are presented in Table 2.

Experiments with seasonal feeding flux. These experiments have seasonal variability of the POM flux. The term "seasonality" is limited to intraannual periods with low and high feeding fluxes. Therefore, to keep the model simple, the seasonality as a complex multivariate phenomenon is reduced to a single variable that is food [57]. Every year is divided into 9 months of low POM flux and 3 months of high POM flux that resemble fertile spring seasons of algal blooms bringing about a high POM flux. Four pairs of POM flux values are tested, they are presented in Table 2.

Description of results. The total amount of nutrients per year (POM flux) is the same for the corresponding constant and seasonal experiments. Simulation results show a clear relationship of the increasing population size with the increasing supply of nutrients.

The most extreme examples are presented on Figs. 9 and 10. The lowest annual feeding flux represented by its constant values of 98.0 μg C_{org} per month sustains extremely oscillating populations of haploids (megalospheric forms) from 0 to 500 living individuals and diploids from 0 to 115 individuals (Fig. 9). The highest feeding flux with constant values of 784.1 μg C_{org} per month maintains from 0 up to 2000 haploid as well as diploid individuals (Fig. 10). When the total number of fossilized shells from 10 experimental years is calculated, haploid (megalospheric) shells dominate (67%) in the experiments with the lowest constant POM fluxes (Fig. 11). The opposite trend is present in experiments with the high constant POM fluxes, where microspheric shells of diploid individuals outnumber (70%) the overall foraminiferal assemblage (Fig. 11).

Experiments with seasonal feeding cycles show much more extreme values of living individuals. Foraminifers reveal the highest number of individuals in fertile 3-month seasons,

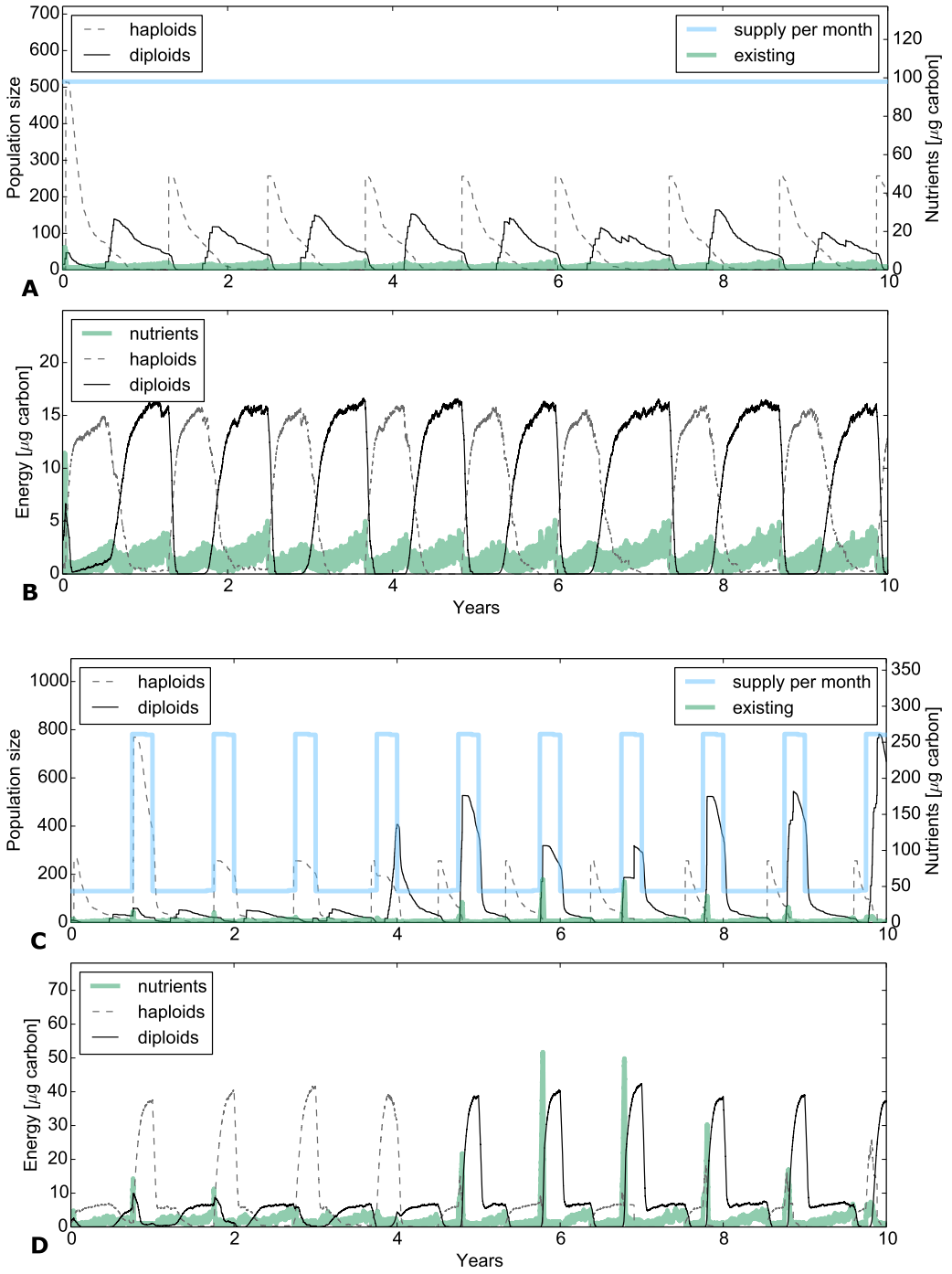

Figure 9: Population dynamics of foraminifera (A, C) and energy carried by each population (B, D) presented per 100 cm^2 in time series of diploid and haploid generations. The total POM flux of 1176.2 μg C_{org} per year is the same for constant (A, B) and seasonal (C, D) feeding experiments. The constant POM flux is 98 μg C_{org} per month (A, B). The seasonal POM flux is 261.38 μg C_{org} per month during 3 months of high (rich) seasons and 43.56 μg C_{org} per month during 9 months of low (poor) seasons (C,D).

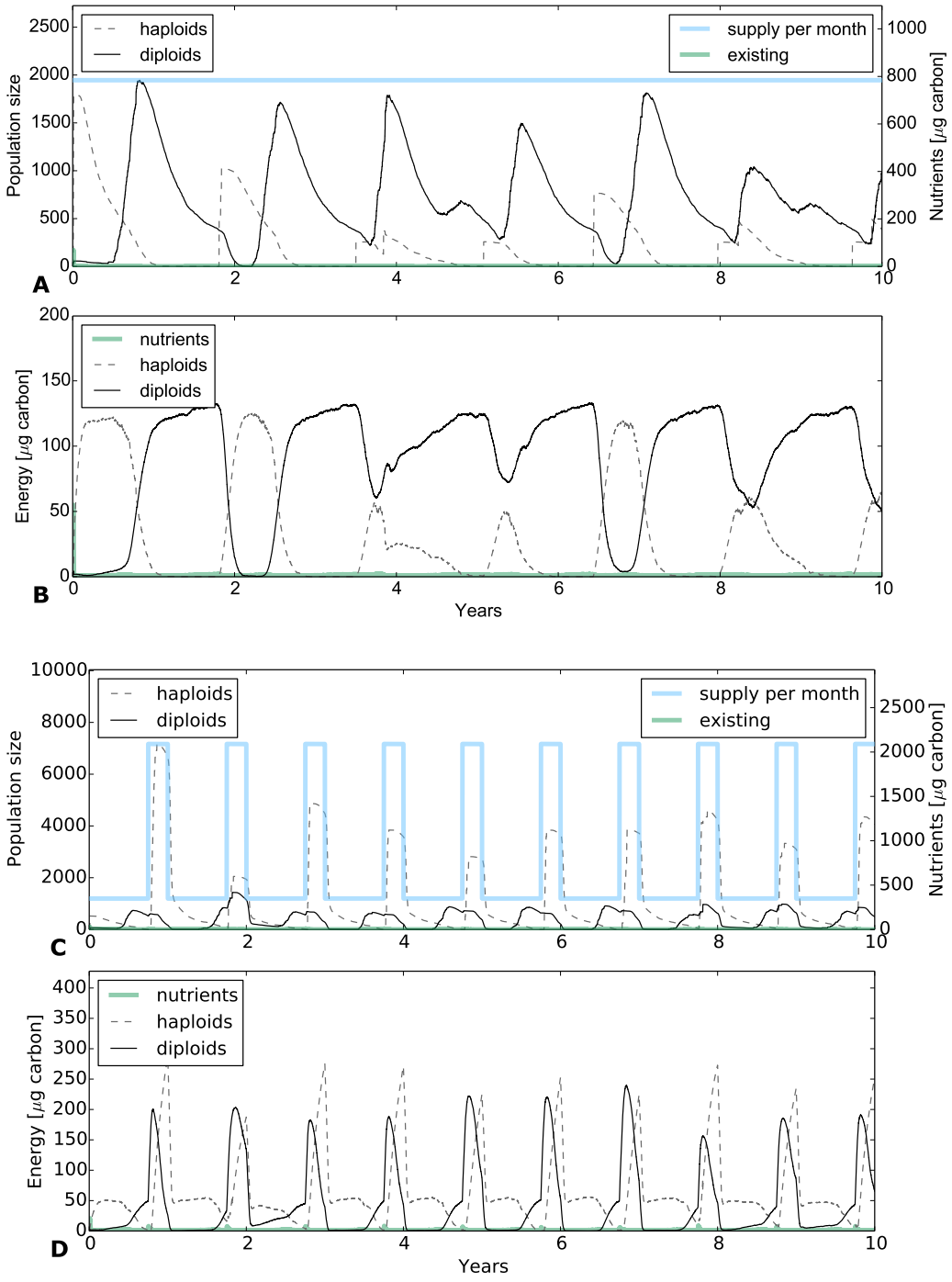

Figure 10: Population dynamics of foraminifera (A, C) and energy carried by each population (B, D) presented per 100 cm^2 in time series of diploid and haploid generations. The total POM flux of 9409.6 μg C_{org} per year is the same for constant (A, B) and seasonal (C, D) feeding experiments. The constant POM flux is 784.1 μg C_{org} per month (A, B). The seasonal POM flux is 2091.04 μg C_{org} per month during 3 months of high (rich) seasons and 348.51 μg C_{org} per month during 9 months of low (poor) seasons (C,D).

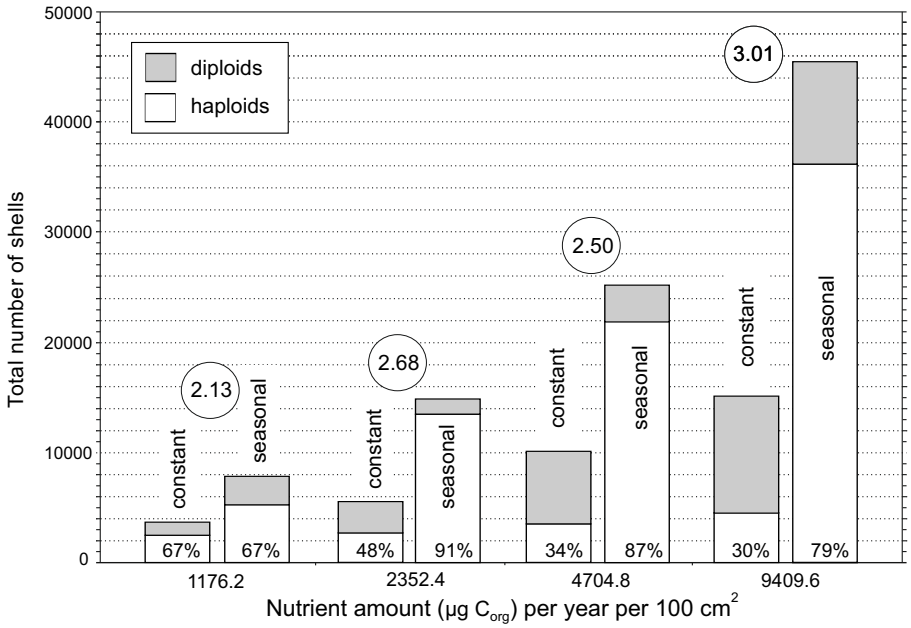

Figure 11: Mean total number of recorded (fossilized) foraminifera, including haploids (megalospheric shells) and diploids (microspheric shells) generated in experiments with constant and seasonal feeding modes. This number of shells represents the number of individual "deaths" either due to shortage of food or reproduction. The experiments simulated 10 years for 4 nutritional levels (see Table 2) and results were averaged from 10 independent runs. The amount of nutrients deposited during one year is the same in both constant and seasonal feeding modes. Numbers in circles are ratios between the total number of shells produced in seasonal and in constant feeding modes.

i.e. max. approximately 800 individuals under the lowest feeding flux (Fig. 9), up to approximately 7000 individuals under the highest feeding flux (Fig. 10). Haploid and diploid individuals do not demonstrate a clear tendency to dominate all fertile (high POM flux) seasons in experiments with the low total annual POM flux of 1176.2 μg C_{org} per year. There are series of fertile seasons dominated either by haploid or diploid individuals (Fig. 9). Experiments with the highest total flux of 9409.6 μg C_{org} per year have revealed populations dominated by haploids during fertile seasons, up to approximately 7000 individuals. Diploids tend to show lower abundances with the oblate maxima at the end of low POM flux seasons and in the beginning of high flux seasons. If the dynamics of energy stored in diploid and haploid individuals is compared, both peaks show a similar range of values (Fig. 10D). This means that lower numbers of diploid individuals are compensated by their larger sizes that store more organic carbon within larger shells.

The most striking feature is the total number of shells in constant feeding compared to seasonal feeding experiments. Fig. 11 collates the mean total number of shells accumulated in every experiment during 10 experimental years. The total number of produced shells is much higher in seasonal experiments. The experiments with the lowest annual POM flux produce 2.13 times more shells during seasonal than constant feeding simulations. This ratio grows to the range from 2.50 to 3.01 in simulations with higher total annual POM fluxes.

In summary, intraannual variability of the food (POM) flux has a direct impact on productivity of foraminifera. The seasonal feeding flux results in much higher frequencies of the same species under the same annually averaged food influx. Therefore, the quantity of food flux as well as its temporal availability pattern strongly affect population dynamics of foraminifera.

The analysis of population dynamics under constant feeding fluxes shows regular oscillations in abundance of macrospheric (haploid) and megalospheric (diploid) generations of foraminifera. These pronounced periodicities are represented by alternating maxima of both generations. Simulations with the low annual feeding flux depict 1.25-year periodicities, so there are 8 alternating haploid and 5 diploid maxima during 10 years of every simulation run (Figs. 9). The high annual feeding flux generates 1.66-year periodicities with approximately 6 alternating haploid and 5 diploid maxima during 10 simulation years (Fig. 10).

When looking at energy flow dynamics, the waves of energy allocation in different generations show similar periodicities, but reveal shifted maxima (Figs. 9 and 10) that are distinctly delayed. The maxima of population size precede maxima of energy allocation in both haploid and diploid populations. This is caused by the maturation of individuals and dramatic shortage of food availability that, in consequence, increases their mortality. A limited number of individuals cross the maturation checkpoint and become ready for reproduction. In some cases, just single individuals of diploids are able to mature and undergo asexual reproduction (Fig. 6). Such reproductions are responsible for forcing alternating cycles of population dynamics of both generations (Figs. 9 and 10).

The analysis of population dynamics under the seasonal feeding mode shows nearly ideal temporal tuning of the foraminiferal population size to seasonal POM flux changes (Figs. 9 and 10). Megalospheric haploids strongly dominate in most fertile seasons with some instabilities in experiments with the lowest annual POM flux. Shells of haploid individuals dominate the assemblage and range from 67 to 91%. These rich seasons are extremely productive because both generations show their highest absolute abundances at the same time. We do not see alternating peaks of absolute abundances of diploid and haploid generations that is in contrast to simulations with the constant feeding flux. Seasons with the low POM flux are much longer and support a lower foraminiferal productivity. Energy flow dynamics follow the population size dynamics in seasonal simulations, although the simulation with the lowest annual feeding flux reveals more complex patterns with additional fluctuations during starvation seasons (Fig. 9).

All simulations present similar proportions of haploids to diploids. Nevertheless, a clear pattern can be seen when constant and seasonal feeding experiments are collated. Seasonal simulations have revealed 67% to 91% of megalospheric shells representing "fossilized" haploid individuals vs. 9% to 33% of microspheric shells that are remnants of diploid individuals. These are global proportions accumulated in 10 simulated years and averaged from 10 experimental runs.

In contrast, simulations under the constant feeding mode reveal a larger range of proportions from 30% to 67% of megalospheric shells (haploids) with a clear tendency to decrease the proportion of these shells with a higher feeding flux (Fig. 11). Therefore, the proportion of microspheric shells (diploids) is positively correlated with higher availability of food.

3.3. Different energy transfer rates

Energy transfer from a food source to an individual is a complex phenomenon. Its rate depends strongly on various intrinsic factors (e.g., enzymes) as well as environmental parameters such as temperature, oxygenation, and the type of organic matter available [49].

In our simulation experiments, we compared $energy\_transfer\_rate = 0.001$ (higher) and 0.0001 (lower). The overall dynamics of haploid and diploid populations was similar for both energy transfer rates. However, for the energy transfer rate equal to 0.0001 and the constant flux mode, there were less reproduction events, and these events produced higher numbers of young diploids (Fig. 12 (A,E)). At the same time, the maximum energy levels carried by the populations of haploids and diploids were the same for both $energy\_transfer\_rate$ values (Fig. 12 (B,F)). This means that in case of the lower energy transfer, the number of

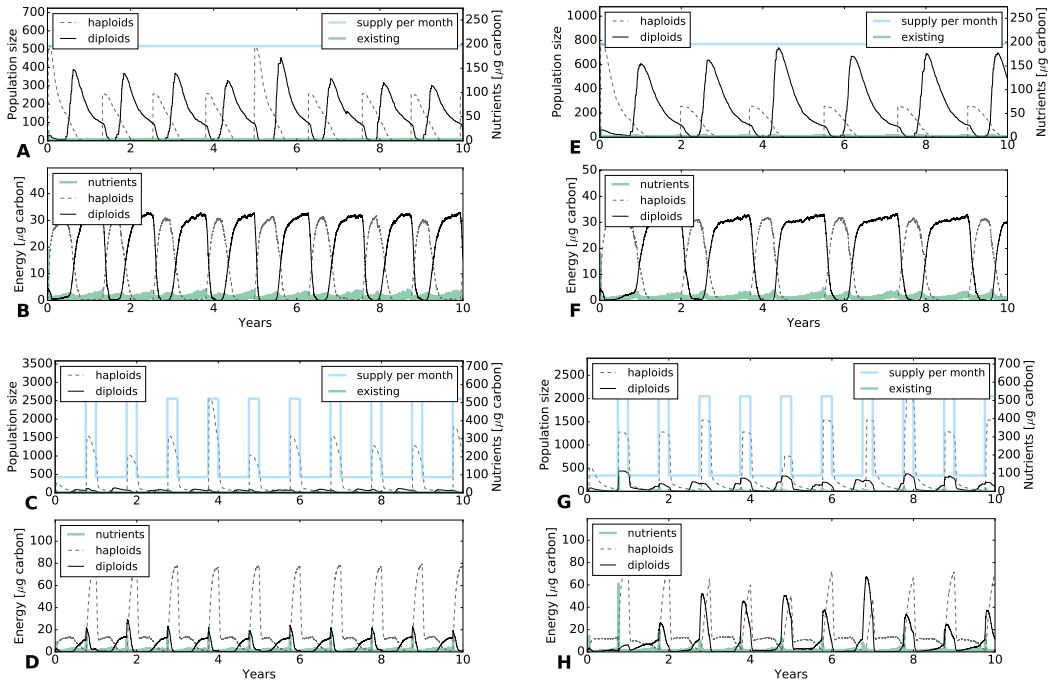

Figure 12: The impact of energy transfer rates on population dynamics of foraminifera (A, C, E, G) and energy carried by each population (B, D, F, H) presented per 100 cm^2 in time series of diploid and haploid generations. Left (A–D): $energy\_transfer\_rate = 0.001$; Right (E–H): $energy\_transfer\_rate = 0.0001$. The total POM flux of 2352.40 μg C_{org} per year is the same for constant (A, B, E, F) and seasonal (C, D, G, H) feeding experiments. The constant POM flux is 196.04 μg C_{org} per month (A, B, E, F). The seasonal POM flux is 522.76 μg C_{org} per month during 3 months of high (rich) season and 87.13 μg C_{org} per month during 9 months of low (poor) season (C, D, G, H).

the young diploids was higher, but their starting energy was lower. In case of the seasonal flux mode, again, the number of the young diploids was higher for the lower energy transfer. The maximum energy level carried by the diploid population is higher for the lower energy transfer rate (Fig. 12 (D,H)).

In general, the overall population dynamics and dependencies between populations were similar for both energy transfer rates. The major differences were the period of fluctuations, the number of offspring, the energy of individuals and the peak population sizes (Fig. 12 (C,G)).

4. Interpretation and discussion

The described experiments present the system where food is the only limiting factor that controls the population size. There is no competition between species because the simulations concern a single species. However, we observe intraspecific competition between individuals and their bimorphic generations. Their energetic trade-offs dependent on fecundity, offspring size, growth rate and maturation checkpoints are responsible for survival and the overall population dynamics.

The total number of recorded (fossilized) foraminifera is proportional to the intensity of food flux. This is observed in all constant and seasonal simulations (Fig. 11). This correlation between the food influx and the overall population size can be interpreted as the consequence of the changing *carrying capacity* of the system (see [58] for an overview of this term). The carrying capacity of the habitat in this case is higher when the POM flux is higher, and if other parameters do not limit the population size. In seasonal habitats, the carrying capacity varies [59] which is expressed by very high fluctuations in abundance of foraminifera (Figs. 9 and 10).

One of the main objectives of this study was to test population dynamics under constant and seasonal feeding regimes with the same annual feeding influx. An interesting finding is that the same amount of food distributed seasonally supports much larger population sizes (Fig. 11). Fertile seasons with a higher feeding flux seem to support much higher numbers of juveniles that come from asexual reproduction, producing megalospheric haploid individuals with large first chambers. Haploid individuals mature earlier, so they live shorter as they are able to grow and reproduce earlier, still within the rich in food season. This reproduction is sexual and produces tiny juveniles that are abundant at the end of rich seasons. Due to abrupt food limitations, their mortality is high; nevertheless, small juveniles leave their record in the virtual fossil record (Fig. 11).

Analogous real cases have been identified in the fossil records from seasonal palaeoenvironments. In the Lower Cretaceous, abundant assemblages of opportunistic foraminifera represented by small benthic species of the *Valvulineria-Gyroidinoides* group were reported [60]. Their abundance correlated well with the Milankovitch obliquity cycles that are known to modulate seasonal contrasts in mid- and high latitudes. The interpretation was that the higher seasonal organic matter fluxes associated with wet seasons were responsible for higher frequencies of small opportunistic foraminifera.

Another study [61] analyzed the Pleistocene quantitative and biometric record of *Epistominella exigua* in the monsoonal Indian Ocean. Higher abundance of *E. exigua* corresponded with smaller shells that had larger proloculi and a smaller number of chambers. This led to the conclusion that the increased abundance of this species was correlated with favorable conditions associated with large seasonal pulses of food supply. This interpretation followed earlier interpretations from similar seasonal environments [16, 62, 63].

Organisms following the r-strategy that are well adapted to abrupt seasonal changes of environmental parameters are called "seasonal opportunists" [64]. R-selective species are

characterized by high productivity, quick reproduction, high fecundity, small body size, early maturity, rapid development, semelparity (single reproduction) and wide dispersal [65]. Foraminifera often follow the r-selected strategy (e.g., [66, 64]). The simulations presented in this work show that such taxa tend to have lower abundance in harsh seasons, but are able to react to food fluxes immediately via a very efficient asexual reproduction mode. The megalospheric (haploid) generation is better adapted to compete for food because their juveniles are larger (the proloculus has a larger radius). However, it is worthwhile to emphasize that the same taxon is able to live under stable nutrient availability as demonstrated by our experiments with a constant feeding flux. Such conditions induce a different population dynamics (Figs. 9 and 10) with a lower total abundance of fossilied shells (Fig. 11).

Seasonal opportunists seem to be widespread in all seasonal climates, from monsoonal low latitudes, through mid latitudes to strongly seasonal high latitudes of the global ocean. Gooday and Rathburn [17] call them "phytodetritus species" that undergo rapid population increase when exposed to pulsed fluxes of phytodetritus. Culture experiments proved such a rapid population response of selected opportunistic taxa to algal phytodetritic pulses [67, 28]. This response is simulated in the seasonal experiments that closely resemble deep ocean assemblages under a permanent shortage of food interrupted by seasonal phytodetritus fluxes [16, 17, 68].

The main problem with the fossil record is that the extraction of seasonality data from time-averaged samples covering hundreds or thousands of years is nontrivial. However, there are characteristic foraminiferal assemblage patterns, such as high abundances of small individuals dominating certain fossil assemblages. Such features can be used for paleoenvironmental interpretations. Understanding these patterns needs long term *in situ* experiments and observations that are not accessible in real time. Our simulation model provides a novel approach to untangle averaged fossil records of population dynamics as a combined response to genetically coded life history strategies and environmental conditions.

All organisms, including Foraminifera, show extremely diverse life history strategies (for overview see [69, 70]). The model described in this work is dedicated to test the adaptability of life history strategies to changing environmental conditions. Such experiments should take into account genetic and evolutionary rules that will be implemented in the future to study evolutionary trade-offs controlling life strategies. Initial implementations of simplified genetic mechanisms have already been tested based on a similar foraminiferal model [71].

There are other intentional limitations of the model introduced here. First of all, it is based just on globothalamean shell morphologies. Therefore, it should be applied to foraminifera with globular chambers that follow different than tubothalamean growth patterns [9]. Another limitation is the simplification of the foraminiferal microhabitat that is restricted to a flat hard bottom without any soft sediments penetrated by infaunal foraminifera. Infaunal (endobenthic) foraminifera tend to respond slower to organic matter fluxes because the organic matter is deposited at the sediment-water interface. The model does not take into account the oxygenation level that controls respiration and metabolic efficiency of foraminifera. Oxygenation, inversely linked to the influx of organic matter, also controls the abundance of foraminiferal populations [6, 27]. New biological and ecological parameters will be implemented in the future to extend the applicability of the model to more complex, realistic scenarios.

5. Conclusions and future prospect

The new simulation tool employed in this work offers a flexible experimental design to run sophisticated *in silico* simulations that can be observed, recorded, and analyzed. This facilitates controlling all foraminiferal growth stages, including juveniles that are neither

recorded in oceanographic procedures, nor extracted from the fossil record. The dynamics of juvenile stages in foraminifera are essential to understand population dynamics as well as spatial and temporal complexity of proxy patterns. Additionally, our approach offers a novel methodology for testing the sensitivity of recent foraminiferal assemblages to pollution and environmental changes. Therefore, it offers predictive applications that allow to simulate various scenarios for monitoring studies. An increased organic matter flux is characteristic for polluted shallow marine basins that often show specific opportunistic reactions of selected species [66, 72].

The development and the implementation of the simulation model required its calibration and testing. Simulated foraminifera and their response to environmental feeding fluxes show realistic patterns known from empirical culture experiments, and oceanographic and paleoecological studies. The variability of annual food flux has a direct impact on the productivity of foraminifera. Population sizes are proportional to the intensity of constant and seasonal food fluxes. This correlation between the food influx and population size is the consequence of the changing carrying capacity of the simulated environment. The carrying capacity of the habitat is higher when the feeding influx is higher as long as other parameters do not limit the population size.

The quantity of the food flux as well as its temporal pattern strongly affect population dynamics of foraminifera. Seasonal feeding pulses result in much higher frequencies of the same species under the same annually averaged food influx. The same amount of food, when distributed seasonally, supports much larger population sizes. Simulations with constant feeding fluxes show intrinsic recurrent oscillations of haploid and diploid generations (Figs. 9, 10 and 11).

The energy transfer rate turned out to influence the periodicity and the number of offspring in reproduction events. Lowering the energy transfer rate resulted in longer intervals between reproduction events in constant feeding experiments. It also increased the peak number of diploids in both constant and seasonal feeding experiments. Since the energy transfer from a food source to an individual is still not well understood, combining empirical and simulation experimental approaches may shed a new light on this complex phenomenon.

The Framsticks environment allowed for an efficient simulation, visualization and analyses of a complex collective system of Foraminifera. For larger-scale experiments, it would be beneficial to divide the world space into a 3D grid so that each cell in the grid can be simulated independently in parallel. This would result in migration of foraminifera between cells which may require synchronization and communication between independent processes, so this distributed approach poses some challenges for the future.

Acknowledgments: The authors would like to thank all eVolutus partners and two anonymous reviewers for constructive suggestions and remarks. The research presented in the paper received support from the Polish National Science Center (DEC-2013/09/B/ST10/01734).

References

[1] M. Bedau, Artificial life: organization, adaptation and complexity from the bottom up, Trends in Cognitive Sciences 7 (11) (2003) 505–512.

[2] M. Komosinski, A. Adamatzky (Eds.), Artificial Life Models in Software, 2nd Edition, Springer, London, 2009. doi:10.1007/978-1-84882-285-6.
URL http://www.springer.com/978-1-84882-284-9

[3] P. Pearson, N. Shackleton, M. Hall, Stable isotopic evidence for the sympatric divergence of *Globigerinoides trilobus* and *Orbulina universa* (planktonic foraminifera), Journal of the Geological Society 154 (1997) 295–302.

[4] L. C. Strotz, A. P. Allen, Assessing the role of cladogenesis in macroevolution by integrating fossil and molecular evidence, Proceedings of the National Academy of Sciences 110 (8) (2013) 2904–2909.

[5] E. Boltovskoy, R. C. Wright, Recent Foraminifera, Dr W. Junk b.v. Publishers The Hague, 1976.

[6] J. Murray, Ecology and palaeoecology of benthic foraminifera, Harlow, Essex, England: Longman Scientific and Technical; New York: Wiley, 1991.

[7] M. Brasier, Microfossils, 1st Edition, George Allen and Unwin, London, 1980.

[8] J. Lipps, Fossil Prokaryotes and Protists, Blackwell Science, 1992.

[9] J. Pawlowski, M. Holzmann, J. Tyszka, New supraordinal classification of foraminifera: Molecules meet morphology, Marine Micropaleontology 100 (2013) 1–10.

[10] P. Labaj, P. Topa, J. Tyszka, W. Alda, 2D and 3D numerical models of the growth of foraminiferal shells, in: Proceedings of the 1st International Conference on Computational Science: Part I, Springer-Verlag, 2003, pp. 669–678.

[11] J. Tyszka, P. Topa, A new approach to modeling of foraminiferal shells, Paleobiology 31 (30) (2005) 526–541.

[12] J. Tyszka, Morphospace of foraminiferal shells: results from the moving reference model, Lethaia 39 (1) (2006) 1–12.

[13] M. Kazirod, W. Korczyński, E. Fernández, A. Byrski, M. Kisiel-Dorohinicki, P. Topa, J. Tyszka, M. Komosinski, Agent-oriented foraminifera habitat simulation, Procedia Computer Science 51 (2015) 1062–1071.

[14] P. Topa, M. Komosinski, J. Tyszka, A. Mensfelt, S. Rokitta, A. Byrski, M. Bassara, eVolutus: A new platform for evolutionary experiments, in: R. Wyrzykowski, E. Deelman, J. Dongarra, K. Karczewski, J. Kitowski, K. Wiatr (Eds.), Parallel Processing and Applied Mathematics: 11th International Conference, PPAM 2015, Krakow, Poland, September 6-9, 2015. Revised Selected Papers, Part II, Springer, 2016, pp. 570–580. doi:10.1007/978-3-319-32152-3_53.
URL http://dx.doi.org/10.1007/978-3-319-32152-3_53

[15] P. Topa, M. Komosinski, M. Bassara, J. Tyszka, eVolutus: a configurable platform designed for ecological and evolutionary experiments tested on foraminifera, in: Man–Machine Interactions 4, Springer, 2016, pp. 269–278.

[16] A. J. Gooday, A response by benthic foraminifera to the deposition of phytodetritus in the deep sea, Nature 332 (6159) (1988) 70–73.

[17] A. J. Gooday, A. E. Rathburn, Temporal variability in living deep-sea benthic foraminifera: a review, Earth-Science Reviews 46 (1) (1999) 187–212.

[18] J. Hohenegger, Large Foraminifera: Greenhouse Constructions and Gardeners in the Oceanic Microcosm, Kagoshima University Museum, 2011.

[19] S. Goldstein, Foraminifera: A Biological Overview, Kluwer Academic Publishers, 1999.

[20] M. Komosinski, S. Ulatowski, Framsticks: Creating and Understanding Complexity of Life, in: M. Komosinski, A. Adamatzky (Eds.), Artificial Life Models in Software, Springer, London, 2009, Ch. 5, pp. 107–148.

[21] M. Komosinski, S. Ulatowski, Framsticks web site, http://www.framsticks.com (2016).

[22] M. Komosinski, S. Ulatowski, Genetic mappings in artificial genomes, Theory in Biosciences 123 (2) (2004) 125–137. doi:10.1016/j.thbio.2004.04.002.

[23] M. Komosinski, A. Rotaru-Varga, Comparison of different genotype encodings for simulated 3D agents, Artificial Life Journal 7 (4) (2001) 395–418. doi:10.1162/106454601317297022.

[24] M. Komosinski, G. Koczyk, M. Kubiak, On estimating similarity of artificial and real organisms, Theory in Biosciences 120 (3-4) (2001) 271–286. doi:10.1007/s12064-001-0023-y.

[25] M. Hapke, M. Komosinski, Evolutionary design of interpretable fuzzy controllers, Foundations of Computing and Decision Sciences 33 (4) (2008) 351–367.

[26] W. Jaskowski, M. Komosinski, The numerical measure of symmetry for 3D stick creatures, Artificial Life Journal 14 (4) (2008) 425–443. doi:10.1162/artl.2008.14.4.14402.

[27] F. J. Jorissen, H. C. de Stigter, J. G. Widmark, A conceptual model explaining benthic foraminiferal microhabitats, Marine Micropaleontology 26 (1) (1995) 3–15.

[28] P. Heinz, H. Kitazato, G. Schmiedl, C. Hemleben, Response of deep-sea benthic foraminifera from the Mediterranean Sea to simulated phytoplankton pulses under laboratory conditions, Journal of Foraminiferal Research 31 (3) (2001) 210–227.

[29] J. L. Travis, S. S. Bowser, The motility of foraminifera, Biology of Foraminifera. Academic Press, London (1991) 91–155.

[30] J. L. Travis, R. D. Allen, Studies on the motility of the foraminifera. i. ultrastructure of the reticulopodial network of *Allogromia laticollaris* (Arnold), Journal of Cell Biology 90 (1) (1981) 211–221.

[31] R. Mesibov, G. W. Ordal, J. Adler, The range of attractant concentrations for bacterial chemotaxis and the threshold and size of response over this range weber law and related phenomena, Journal of General Physiology 62 (2) (1973) 203–223.

[32] E. A. Martens, N. Wadhwa, N. S. Jacobsen, C. Lindemann, K. H. Andersen, A. Visser, Size structures sensory hierarchy in ocean life, in: Proc. R. Soc. B, Vol. 282, The Royal Society, 2015, p. 20151346.

[33] M. R. Langer, C. A. Gehring, Bacteria farming; a possible feeding strategy of some smaller motile foraminifera, Journal of Foraminiferal Research 23 (1) (1993) 40–46.

[34] H. Kitazato, Locomotion of some benthic foraminifera in and on sediments, Journal of Foraminiferal Research 18 (4) (1988) 344–349.

[35] M. Arslan, M. A. Kaminski, A. B. Khalil, Living behaviors of benthic foraminifera from eastern bahrain and the saudi coastline, Bulletin of Environmental Studies 1 (1) (2016) 1–9.

[36] L. Seuront, V. M. Bouchet, The devil lies in details: New insights into the behavioural ecology of intertidal foraminifera, Journal of Foraminiferal Research 45 (4) (2015) 390–401.

[37] M. Putt, D. Stoecker, An experimentally determined carbon: volume ratio for marine "oligotrichous" ciliates from estuarine and coastal waters, Limnology and Oceanography. Wiley 34 (6) (1989) 1097–1103.

[38] W. H. Berger, Planktonic foraminifera: basic morphology and ecologic implications, Journal of Paleontology (1969) 1369–1383.

[39] J. J. Lee, H. D. Freudenthal, W. A. Muller, V. Kossoy, S. Pierce, R. Grossman, Growth and physiology of foraminifera in the laboratory: Part 3: Initial studies of *Rosalina floridana* (Cushman), Micropaleontology (1963) 449–466.

[40] R. Nigam, A. S. Rao, Proloculus size variation in recent benthic foraminifera: Implications for paleoclimatic studies, Estuarine, Coastal and Shelf Science 24 (5) (1987) 649–655.

[41] E. H. Myers, The present state of our knowledge concerning the life cycle of the foraminifera, Proceedings of the National Academy of Sciences 24 (1) (1938) 10–17.

[42] S. T. Goldstein, W. W. Barker, Gametogenesis in the monothalamous agglutinated foraminifer *Cribrothalammina alba*, Journal of Protozoology 37 (1) (1990) 20–27.

[43] R. Röttger, C. Dettmering, R. Krüger, R. Schmaljohann, J. Hohenegger, Gametes in nummulitids (Foraminifera), Journal of Foraminiferal Research 28 (4) (1998) 345–348.

[44] E. Alve, S. T. Goldstein, Dispersal, survival and delayed growth of benthic foraminiferal propagules, Journal of Sea Research 63 (1) (2010) 36–51.

[45] S. T. Goldstein, E. Alve, Experimental assembly of foraminiferal communities from coastal propagule banks, Marine Ecology Progress Series 437 (2011) 1–11.

[46] F. Hannah, R. Rogerson, J. Laybourn-Parry, Respiration rates and biovolumes of common benthic foraminifera (Protozoa), Journal of the Marine Biological Association of the United Kingdom 74 (02) (1994) 301–312.

[47] I. Hecht, S. Natan, A. Zaritsky, H. Levine, I. Tsarfaty, E. Ben-Jacob, The motility-proliferation-metabolism interplay during metastatic invasion, Scientific reports 5.

[48] R. W. Angell, Calcification during chamber development in rosalina floridana, Journal of Foraminiferal Research 9 (4) (1979) 341–353.

[49] J. A. Tuszynski, M. Kurzynski, Introduction to Molecular Biophysics, CRC Press, 2003.

[50] J. J. Lee, W. A. Muller, Trophic dynamics and niches of salt marsh foraminifera, American zoologist 13 (1) (1973) 215–223.

[51] D. R. Levitan, M. A. Sewell, F.-S. Chia, How distribution and abundance influence fertilization success in the sea urchin *Strongylocentotus franciscanus*, Ecology (1992) 248–254.

[52] E. A. Serrao, G. Pearson, L. Kautsky, S. H. Brawley, Successful external fertilization in turbulent environments, Proceedings of the National Academy of Sciences 93 (11) (1996) 5286–5290.

[53] O. Kaplan, M. Firon, A. Vivi, G. Navon, et al., Hgf/sf activates glycolysis and oxidative phosphorylation in da3 murine mammary cancer cells, Neoplasia 2 (4) (2000) 365–377.

[54] J. Erez, A. Almogi-Labin, S. Avraham, On the life history of planktonic foraminifera: lunar reproduction cycle in *Globigerinoides sacculifer* (brady), Paleoceanography 6 (3) (1991) 295–306.

[55] R. A. Ims, The ecology and evolution of reproductive synchrony, Trends in Ecology & Evolution 5 (5) (1990) 135–140.

[56] M. Komosinski, A. Mensfelt, P. Topa, J. Tyszka, S. Ulatowski, Foraminifera: genetics, morphology, simulation, evolution, http://www.framsticks.com/foraminifera (2016).

[57] M. S. Boyce, Seasonality and patterns of natural selection for life histories, American Naturalist (1979) 569–583.

[58] D. Price, Carrying capacity reconsidered, Population and Environment 21 (1) (1999) 5–26.

[59] B. Wilson, B. P. Horton, Determining carrying capacity from foraminiferal time-series, Journal of Micropalaeontology 31 (2) (2012) 111–119.

[60] J. Tyszka, Foraminiferal response to seasonality modulated by orbital cycles in the Cretaceous mid-latitudes: the Albian record from the Lower Saxony Basin, Palaeogeography, Palaeoclimatology, Palaeoecology 276 (1) (2009) 148–159.

[61] R. Saraswat, A. Deopujari, R. Nigam, P. Heniriques, Relationship between abundance and morphology of benthic foraminifera *Epistominella exigua*: Paleoclimatic implications, Journal of the Geological Society of India 77 (2) (2011) 190–196.

[62] A. J. Gooday, Deep-sea benthic foraminiferal species which exploit phytodetritus: characteristic features and controls on distribution, Marine Micropaleontology 22 (3) (1993) 187–205.

[63] A. K. Gupta, E. Thomas, Initiation of northern hemisphere glaciation and strengthening of the northeast indian monsoon: Ocean drilling program site 758, eastern equatorial indian ocean, Geology 31 (1) (2003) 47–50.

[64] J. Tyszka, Seasonal opportunists: *in fossilio* experiment on Albian foraminifera, in: The Micropalaeontological Society's Foraminifera and Nannofossil Groups' Joint Spring Meeting, Micropalaeontological Society, London, 2010, pp. 9–10.

[65] E. R. Pianka, On r- and K-selection, American Naturalist 104 (940) (1970) 592–597.

[66] E. Alve, A common opportunistic foraminiferal species as an indicator of rapidly changing conditions in a range of environments, Estuarine, Coastal and Shelf Science 57 (3) (2003) 501–514.

[67] J. S. Bradshaw, Laboratory experiments on the ecology of foraminifera, Contributions from the Cushman Foundation for Foraminiferal Research (1961) 87–106.

[68] C. Fontanier, F. Jorissen, G. Chaillou, C. David, P. Anschutz, V. Lafon, Seasonal and interannual variability of benthic foraminiferal faunas at 550m depth in the Bay of Biscay, Deep Sea Research Part I: Oceanographic Research Papers 50 (4) (2003) 457–494.

[69] S. C. Stearns, Trade-offs in life-history evolution, Functional Ecology 3 (3) (1989) 259–268.

[70] S. C. Stearns, The evolution of life histories, Vol. 249, Oxford University Press Oxford, 1992.

[71] P. Topa, Ł. Faber, J. Tyszka, M. Komosinski, Modelling ecology and evolution of foraminifera in the agent-oriented distributed platform, Journal of Computational Science.

[72] E. Alve, S. Korsun, J. Schönfeld, N. Dijkstra, E. Golikova, S. Hess, K. Husum, G. Panieri, Foram-ambi: A sensitivity index based on benthic foraminiferal faunas from north-east atlantic and arctic fjords, continental shelves and slopes, Marine Micropaleontology 122 (2016) 1–12.